Supplementary Materials

Adsorption of cationic/anionic dyes and endocrine disruptors by yeast/cyclodextrin polymer composites

Zhikun Lv [a], Zhaoyang Wang[a], Huaiguang Wang[a], Liang Chen[a], Yuhao Hao[a], Ruoxuan Li[a], Jianbin Li[a, b, c,*], Kai Li [a, b, c,*]

[a] College of Light Industry and Food Engineering, Guangxi University, Nanning 530004, Guangxi, China;

[b] Provincial and Ministerial Collaborative Innovation Center for Sugar Industry, Nanning 530004, China;

[c] Engineering Research Center for Sugar Industry and Comprehensive Utilization, Ministry of Education, Nanning 530004, China

* Corresponding authors:

Tel.: +86 13978609908 (Jianbin Li)

+86 13877115103 (Kai Li)

E-mail addresses: lijb0771@sina.com (Jianbin Li); gxlikai@gxu.edu.cn (Kai Li)

S1. Methods

S1.1. Characterization method

Fourier transform infrared spectroscopy (FTIR; IRTracer-100, Shimadzu, Japan) was used to detect the surface functional groups on the materials. A Bruker D8 X-ray diffractometer goniometer (XRD; A24A10, Bruker AXS GMBH, Germany) was used to examine the structure and crystallinity of the samples. Scanning electron microscopy (SEM; Zeiss Gemini 3000, Carl Zeiss, Germany) was used to determine the morphology of IBY and IBY-PA-CDP. The zeta potentials of the materials at pH = 2–11 were measured using a nanoparticle size and zeta potential analyzer (Nano-ZS90X, Malvern, UK). X-ray photoelectron spectroscopy (XPS; K-Alpha, Thermo Fisher Scientific, USA) was used to determine the changes in the surface elements of the materials. The static contact angles of IBY and IBY-PA-CDP were measured using a contact angle meter (DSA100, KRUSS, Germany).

S1.2. Batch adsorption experiment

The performances of the adsorbents for MB/BPA/MO removal were investigated using batch adsorption experiments. Experiments were conducted at different concentrations of 200–750 mg/L MB solution, 20–100 mg/L BPA solution and 20–160 mg/L MO solution. The pH of the solution was adjusted and 15 mL of the solution was pipetted into a 50 mL conical flask to which different doses of IBY-PA-CDP (0.6–1.6 g/L) were added. The conical flasks were then placed in a digital speed-measuring thermostatic shaker at 150 rpm, temperature was adjusted (288–328 K), and concentrations of the solutions were measured at specified time (3–1200 min).

The effects of salts and humic acid on the adsorption efficiencies of the modeled pollutants were also investigated. Moreover, changes in the adsorption of MB/BPA/MO in a binary system of simulated pollutants were systematically investigated. Once the aforementioned adsorption experiments reached the set time, the solutions were filtered through a 0.22 μm filter membrane, and the absorbance values of MB (665 nm), BPA (276 nm), and MO (464 nm) were determined using a UV spectrophotometer.

The specific experimental conditions for investigating the effect of pH were as follows: for IBY, 80 mg/L MB, 30 mg/L BPA/MO; for IBY-PA-CDP, 600 mg/L MB, 50 mg/L BPA/MO; temperature, 298 K; dosage, 1.0 g/L; time, 20 h.

Specific experimental conditions for investigating the effect of temperature: IBY-PA-CDP: pH=11, 600 mg/L MB; pH=7, 50 mg/L BPA; pH=3, 50 mg/L MO; dosage, 1.0 g/L; time = 20 h.

The specific experimental conditions for investigating the effect of dosage were as follows: IBY-PA-CDP, pH=11, 600 mg/L MB; pH=7, 50 mg/L BPA; pH=3, 50 mg/L MO; temperature, 298 K; and time, 20 h.

The specific experimental conditions for investigating the effect of contact time were as follows: IBY-PA-CDP, pH=11, 600 mg/L MB; pH=7, 50 mg/L BPA; pH=3, 50 mg/L MO; temperature = 298 K; and dosage, 1.0 g/L.

The specific experimental conditions for investigating the effect of ionic strength and humic acids on IBY-PA-CDP were as follows: pH=11, 200 mg/L MB; pH=7, 50

mg/L BPA; pH=3, 50 mg/L MO; temperature = 298 K; dosage, 1.0 g/L; and time = 20 h.

Specific experimental conditions for investigating the effect of strong/weak acidic ionic salts: for IBY-PA-CDP, pH=3, 50 mg/L MO; temperature, 298 K; dosage, 1.0 g/L; and time, 20 h. We used 0.05 mol/L of NaCl, $NaNO_3$, Na_2SO_4, CH_3COONa, and $NaH_2PO_4 \cdot 2H_2O$.

Specific experimental conditions for investigating the effect of metal ions: for IBY-PA-CDP, pH=4, 200 mg/L MB; temperature, 298 K; dosage, 1.0 g/L; and time, 20 h. We used 0.005 mol/L KCl, $CaCl_2$, $MnSO_4 \cdot 7H_2O$, and $CuSO_4 \cdot 5H_2O$.

The specific experimental conditions to investigate the effect of pH on each pollutant in the binary system were as follows: IBY-PA-CDP, 50 mg/L BPA, 50/100 mg/L MB, 50 mg/L BPA, 30/60 mg/L MO, 50 mg/L MO, 50/100 mg/L MB; temperature, 298 K; dosage, 1.0 g/L; time, 20 h.

The concentration of MB/BPA/MO in the remaining solution was calculated from the absorbance value of the solution following adsorption of the target pollutant by IBY-PA-CDP. The adsorption capacity q_t of MB/BPA/MO at time t, adsorption capacity q_e at equilibrium, and removal efficiency η were obtained using Eqs. (S1), (S2), (S3).

$$q_t = \frac{(C_0 - C_t) \times V}{m} \quad \text{(S1)}$$

$$q_e = \frac{(C_0 - C_e) \times V}{m} \quad \text{(S2)}$$

$$\eta = \frac{C_0 - C_e}{C_0} \times 100\% \quad \text{(S3)}$$

where q_t represents the adsorption capacity of the adsorbate on the adsorbent at time t (mg/g); C_0 and C_t denote the initial concentration of the adsorbent and the residual concentration of the adsorbent at time t (mg/L), respectively; V denotes the volume of adsorbate solution (L); m denotes the amount of the adsorbent added (g); q_e denotes the adsorption capacity of the adsorbate on the adsorbent adsorption equilibrium (mg/g); C_e is the remaining concentration of the adsorbate in the solution at adsorption equilibrium (mg/L); η denotes the removal rate of the adsorbate on the adsorbent.

S1.3. Adsorption kinetics

To reveal the adsorption properties (chemical/physical adsorption) of MB/BPA/MO onto IBY-PA-CDP, adsorption kinetics were used to fit the experimental data. Adsorption kinetic studies also provided information on the rate of adsorption. In the present study, several kinetic models were used to fit the kinetic data, including the pseudo-first-order (PFO), pseudo-second-order (PSO), and Elovich models.

The PFO kinetic model considers the adsorption process to be physisorption, using Eq. (S4):

$$q_t = q_e\left(1 - e^{-k_1 t}\right) \quad \text{(S4)}$$

where k_1 (1/min) is the rate constant of the PFO kinetic model.

The PSO kinetic model was used to describe adsorption as chemisorption,[1] as

shown in Eq. (S5):

$$q_t = \frac{{q_e}^2 k_2 t}{1 + q_e k_2 t} \quad \text{(S5)}$$

where k_2 (g/(mg·min)) is the rate constant of the PSO model.

The Elovich kinetic model shows that inhomogeneous chemical adsorption occurs on the adsorbent surface and that the activation energy increases with time. The Elovich kinetic model is expressed by Eq. (S6) [2]:

$$q_e = \frac{1}{b} ln(1 + abt) \quad \text{(S6)}$$

where a and b are the adsorption rate [mg/(g·min)] and desorption rate constant (g/mg), respectively.

S1.4. Adsorption isotherms

Isotherm modeling of the adsorbent and adsorbent mass equilibrium data can predict the maximum adsorption capacity during adsorption. In addition, adsorption isotherm modeling can describe the form of adsorption of an adsorbate on the adsorbent mass (monolayer/multilayer adsorption) at a constant temperature. Classical models of adsorption isotherms, including the Langmuir, Freundlich, and Temkin models, are often used to fit experimental curves.

The Langmuir isotherm model describes the monolayer adsorption with a uniform distribution of adsorption sites using the following equation:

$$q_e = \frac{q_m K_L C_e}{1 + K_L C_e} \quad \text{(S7)}$$

where q_m (mg/g) is the maximum capacity, and K_L (L/mg) is the Langmuir model coefficient.

To assess whether the Langmuir isotherm model was favorable for adsorption, the separation factor R_L, as shown in Eq. (S8):

$$R_L = \frac{1}{1 + K_L C_0} \quad \text{(S8)}$$

where C_0 is the initial concentration and R_L is a dimensionless constant. When $R_L = 0$, adsorption is irreversible. For values between $0 < R_L < 1$, the adsorption process is indicated to be favorable. $R_L = 1$ indicates a linear biosorption process, and $R_L > 1$ indicates that the biosorption process is unfavorable.

The Freundlich isotherm model describes multimolecular layer adsorption with heterogeneous surface properties using Eq. (S9):

$$q_e = K_F C_e^{\frac{1}{n}} \quad \text{(S9)}$$

where K_F is the Freundlich constant ((mg/g)(L/mg)$^{1/n}$), and n is the adsorption strength parameter of the Freundlich equation. The strength of adsorption or surface heterogeneity is denoted by 1/ n, which indicates the relative distribution of the energy and heterogeneity of the adsorbate sites. Adsorption is favorable when 1/ n is greater than 0 ($0 < 1/ n < 1$), unfavorable when 1/ n is greater than 1, and irreversible when $1/ n = 1$.

The Temkin isotherm model also describes multilayer adsorption behavior; however, it considers the effect of the heat on adsorption.[3] It also showed a linear

decreasing trend in the biosorption energy change rather than an exponential decreasing trend, as in the Freundlich isotherm. The Temkin isotherm model can be described using Eq. (S10) [4]:

$$q_e = \frac{RT}{b}\ln\left(AC_e\right) \quad \text{(S10)}$$

where b is the Temkin isotherm constant (J/mol), A is the binding constant at equilibrium (L/g), R is the gas constant 8.314 (J/mol/K), and T is the absolute temperature (K).

S1.5. Adsorption thermodynamics

Thermodynamic parameters were calculated using the Van't Hoff equation from the adsorption capacity and equilibrium concentration of IBY-PA-CDP on MB/BPA/MO at different temperatures. ΔG, ΔH, and ΔS were used to determine the spontaneity, nature, and correlation of adsorption, respectively, elucidating the thermodynamic behavior of adsorption.[5]

$$\Delta G = \Delta H - T\Delta S = -RTlnK \quad \text{(S11)}$$

$$lnK = \frac{-\Delta H}{RT} + \frac{\Delta S}{R} \quad \text{(S12)}$$

$$K = \frac{q_e}{C_e} \quad \text{(S13)}$$

where ΔG, ΔH, and ΔS are the standard free energy (kJ/mol), enthalpy change (kJ/mol), and entropy change [J/(mol·K)], R is the universal gas constant [8.314 J/(mol·K)], and K is the distribution coefficient (L/g). Van't Hoff plots were made

with 1/T and lnK plotted as the horizontal and vertical coordinates respectively, and the values of ΔH and ΔS were obtained from the slopes and intercepts on the curves.

S1.6. Regeneration

The adsorbents loaded with MB, MO, and BPA were eluted using 100 mL of CH_3CH_2OH/HCl, CH_3OH/NaOH (0.2 mol/L), and 50 mL of CH_3OH, respectively. The elution process was repeated thrice for 2 h. Then, the desorbed adsorbent was separated again, washed thrice with deionized water to remove the residual eluate, and dried. The regenerated adsorbent was reused for adsorption experiments, and the removal rate was evaluated for five consecutive adsorption-desorption cycles.

S2. Results and discussion

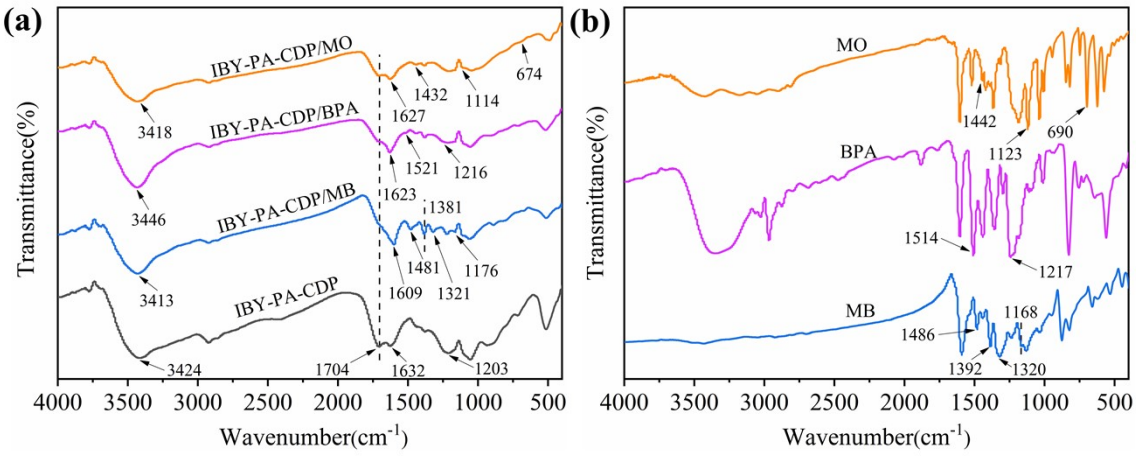

Fig. S1. (a) FTIR spectra of IBY-PA-CDP loaded with MB, BPA, and MO; (b) FTIR spectra of MB, BPA, and MO.

Fig. S1a presents the FTIR spectroscopy of IBY-PA-CDP before and after loading MB/BPA/MO. Fig. S1b shows the FTIR spectra of MB, BPA and MO. After the adsorption of MB, the clearer and sharper characteristic peaks appearing near 1481 and 1381 cm^{-1} are the benzene ring-C=C-stretching vibration and the biphenyl

unit, respectively [6] [208]. Furthermore, the peaks at 1321 and 1176 cm^{-1} corresponded to the C-N and N-CH_3 of MB, respectively. After the adsorption of BPA, the absorption peak of the -OH stretching vibration shifted from 3424 to 3446 cm^{-1}, and the increase in the wavenumber was attributed to the BPA molecule (hydroxyl group). The emerging weak peak at 1521 cm^{-1} is attributed to the bending vibration of the aromatic ring C=C bond backbone. Moreover, the shift in the absorption peak from 1203 cm^{-1} to 1216 cm^{-1} is attributed to the phenolic C–O band.[7] After the adsorption of MO, two new peaks 1432, 1114, and 674 cm^{-1} appeared belonging to the characteristic peaks of MO.

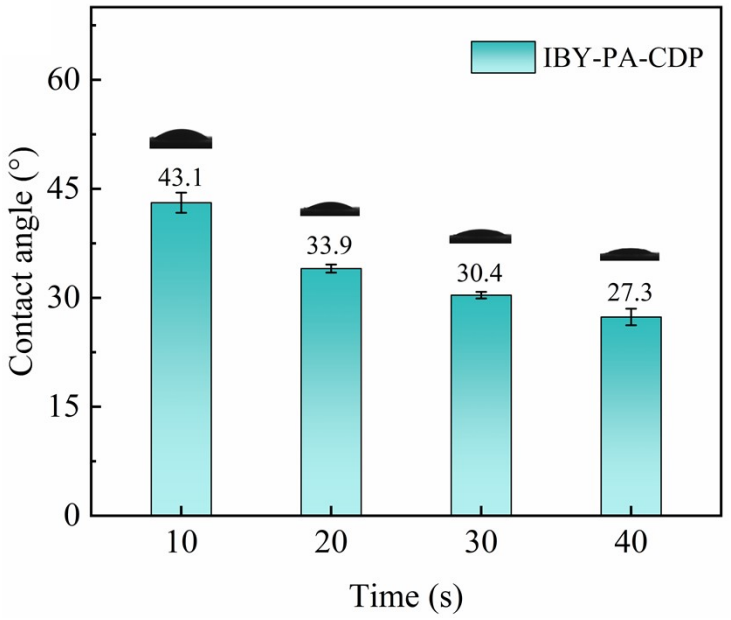

Fig. S2. Static contact angles of IBY and IBY-PA-CDP.

Fig. S3. Photographs of IBY and IBY-PA-CDP.

Table S1 Weight percentage contents of each element of IBY, IBY-PA-CDP and IBY-PA-CDP/model contaminants.

Element	C (%)	N (%)	O (%)	P (%)	S (%)
IBY	45.99 ± 4.16	27.26 ± 1.37	26.36 ± 0.69	0.38 ± 0.02	-
IBY-PA-CDP	42.98 ± 1.91	23.74 ± 2.60	29.61 ± 1.35	3.67 ± 0.51	-
IBY-PA-CDP/MB	49.96 ± 2.63	17.97 ± 0.82	27.76 ± 2.14	2.34 ± 0.42	1.97 ± 0.22
IBY-PA-CDP/BPA	45.40 ± 3.84	15.46 ± 1.05	35.12 ± 3.98	4.02 ± 0.36	-
IBY-PA-CDP/MO	44.80 ± 3.53	15.91 ± 0.71	35.31 ± 2.33	3.85 ± 0.45	0.13 ± 0.01

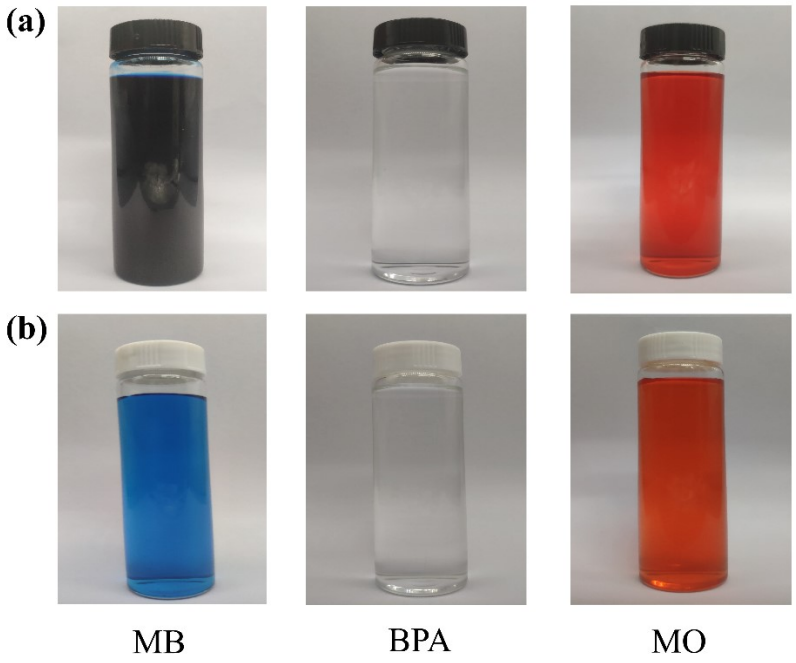

Fig. S4. Macroscopic changes (a) before and (b) after the adsorption of MB, BPA, and MO by IBY-PA-CDP (pH 11, 600 mg/L MB; pH 7, 50 mg/L BPA; pH 3, 50 mg/L MO; temperature, 298 K; dosage, 1.0 g/L; time, 20 h.)

Adsorption thermodynamics

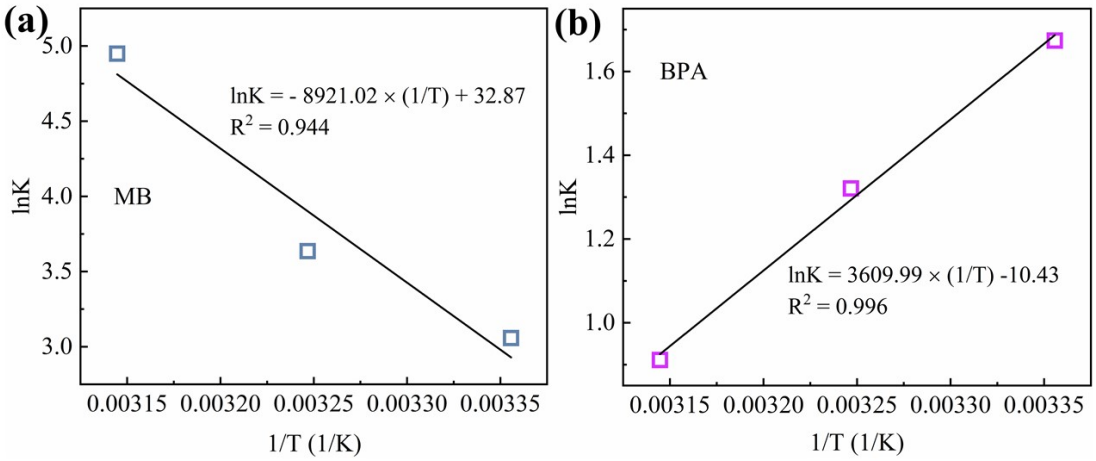

Fig. S5. Fitting curves for thermodynamic of MB (a), BPA (b) and MO (c) adsorbed by IBY-PA-CDP.

The values of the thermodynamic parameters in Table S2 were obtained from the curvilinear equations in Fig. S5. The negative value of Δ*G* demonstrates that the removal of MB/BPA/MO from IBY-PA-CDP was a spontaneous process. Whereas, the Δ*G* value (0.05 kJ/mol) is positive for MO at 318 K, which is a non-spontaneous process. The positive value of Δ*H* confirmed that the uptake process of IBY-PA-CDP to MB was adsorptive. On the contrary, the negative value of Δ*H* implies that the removal of BPA and MO is exothermic. Furthermore, the parameter Δ*S* indicate changes in disorder. A positive value of Δ*S* indicates increased disorder during MB uptake.[8] Contrarily, the negative value of Δ*S* of BPA and MO demonstrates a decrease in solid/solution interface disorder during adsorption.[9]

Table S2 Thermodynamic parameters of MB/BPA/MO adsorption by IBY-PA-CDP.

Adsorbate	Temputure (K)	Δ*G* (kJ/mol)	Δ*H* (kJ/mol)	Δ*S* [J/(mol·k)]
MB	298	-7.56	74.17	273.28
	308	-9.31		
	318	-13.08		

BPA	298	-4.15	-30.01	-86.72
	308	-3.38		
	318	-2.41		
MO	298	-0.73	-12.34	-38.99
	308	-0.26		
	318	0.05		

Table S3 Kinetic parameters of MB/BPA/MO adsorption by IBY-PA-CDP.

Adsorbate		MB	BPA	MO
$q_{e,exp}$ (mg/g)		563.06	42.25	28.61
PFO model	$q_{e,cal}$ (mg/g)	510.24	37.73	24.51
	k_1 (1/min)	0.018	0.024	0.011
	R^2	0.906	0.862	0.881
PSO model	$q_{e,cal}$ (mg/g)	554.41	40.19	27.17
	k_2[g/(mg·min)]	0.025	0.039	0.015
	R^2	0.961	0.930	0.938
Elovich model	a[mg/(g·min)]	51.054	9.303	1.233
	b(g/mg)	0.011	0.178	0.210
	R^2	0.994	0.986	0.986

Table S4 Parameters for isotherms of MB/BPA/MO adsorption onto IBY-PA-CDP.

Adsorbate	Langmuir model			Freundlich model			Tempkin model		
	q_m (mg/g)	K_L (L/mg)	R^2	K_F	1/n	R^2	b	A	R^2
MB	630.96	0.89	0.992	327.36	0.17	0.898	30.65	45.38	0.948
BPA	83.31	0.13	0.941	17.31	0.41	0.857	125.01	1.07	0.938
MO	72.71	0.03	0.970	5.72	0.52	0.990	170.51	0.38	0.952

Table S5 Parameters of the EXD, IND, and ADAS models for adsorption of MB and BPA by IBY-PA-CDP.

Adsorbate		MB	BPA
EXD model	$k_{MW}{\cdot}S$ (1/min)	0.01	0.01
	m_v (g/L)	1.00	1.00
	R^2	0.820	0.514
IND model 1	k_1 [mg/(g·min)$^{0.5}$]	35.53	3.30
	R^2	0.947	0.935
IND model 2	k_2 [mg/(g·min)$^{0.5}$]	5.88	0.39
	R^2	0.939	0.976
ADAS model	k_R (1/min)	0.03	0.06
	n	3.29	10.45
	R^2	0.979	0.982

References

1. G. B. Oguntimein, *Journal of Environmental Chemical Engineering*, 2015, **3**, 2647-2661.
2. A. Agarwal, U. Upadhyay, I. Sreedhar, S. A. Singh and C. M. Patel, *Journal of Water Process Engineering*, 2020, **38**, 101602.
3. M. Chen, Z. Yan, J. Luan, X. Sun, W. Liu and X. Ke, *Chem. Eng. J.*, 2023, **454**, 140300.
4. K. Yin, Q. Wang, M. Lv and L. Chen, *Chem. Eng. J.*, 2019, **360**, 1553-1563.

5. X. Guo, Y. Liu and J. Wang, *J. Hazard. Mater.*, 2020, **400**, 123324.
6. S. Y. Yap, S. Sreekantan, M. Hassan, K. Sudesh and M. T. Ong, *Journal*, 2021, **13**.
7. F. M. Mpatani, A. A. Aryee, A. N. Kani, Q. Guo, E. Dovi, L. Qu, Z. Li and R. Han, *Chemosphere*, 2020, **259**, 127439.
8. K. Saini, A. Sahoo, B. Biswas, A. Kumar and T. Bhaskar, *Bioresour. Technol.*, 2021, **342**, 125924.
9. M. Bilal, I. Ihsanullah, M. U. Hassan Shah, A. V. Bhaskar Reddy and T. M. Aminabhavi, *J. Environ. Manage.*, 2022, **321**, 115981.